

# Modelling Collaborative Motion in Mobile Ad-Hoc Networks

Ilyes Boulkaibet (ilyes@aims.ac.za)

إلياس بولكعيبات

African Institute for Mathematical Sciences (AIMS)

Supervised by Anthony E. Krzesinski

University of Stellenbosch

May 24, 2007

# Abstract

This essay explores a model for the operation of an ad hoc network and the effect of the mobile nodes. The model incorporates incentives for users to act as transit nodes on multi-hop paths and to be rewarded with their own ability to send traffic. The essay explores consequences of the model by means of simulation of a network and illustrates the way in which network resources are allocated to user according to their geographical position. The mobile nodes are explored in this essay, where nodes have incentives to collaborate.

## الخلاصة

يدرس هذا العمل نموذجًا لتشغيل شبكة مخصصة و اثر العقد المتحركة عليه. النموذج يتضمن حوافز لمستخدمين كالذين يستعملون كعقد مرور في نظام طرق متعدّدة و الجزاء مع مراعات قدرتها على الإرسال. هذا العمل ايضًا يكشف نتائج النموذج عن طريق محاكاة الشبكة. و يوضح موارد الشبكة و حصة المستخدم وفقًا لموقعه الجغرافي. في هذا العمل، العقد المتحركة موضحة أين العقد محفزة للتعاون.

# Contents

<b>Abstract</b>	<b>i</b>
<b>1 Introduction</b>	<b>1</b>
<b>2 Mobility Model for Ad Hoc Networks</b>	<b>2</b>
2.1 Overview . . . . .	2
2.2 Random Waypoint Model . . . . .	2
2.3 Random Gauss-Markov Model . . . . .	2
2.4 Reference Point Group Mobility . . . . .	3
2.5 Comments . . . . .	5
<b>3 Biological Mobility Models</b>	<b>7</b>
3.1 Overview . . . . .	7
3.2 The Model . . . . .	7
3.3 Analysis of the Model . . . . .	9
<b>4 Incentives for Collaboration</b>	<b>13</b>
4.1 Overview . . . . .	13
4.2 System Description . . . . .	13
4.2.1 Traffic Flow on Routes . . . . .	13
4.2.2 Capacity Constraint . . . . .	14
4.2.3 Energy Management . . . . .	14
4.3 Model . . . . .	15
4.3.1 Dual Algorithm for Flow Allocation . . . . .	15
4.3.2 Balancing the Congestion Costs . . . . .	16
4.4 Simulations . . . . .	17
4.4.1 Static Networks . . . . .	18
4.4.2 Mobile Networks . . . . .	22
4.4.3 Autonomous Network . . . . .	25

<b>5 Conclusion</b>	<b>28</b>
<b>Bibliography</b>	<b>31</b>

# 1. Introduction

A mobile ad hoc network is formed by a set of communicating nodes capable of motion. Some of these mobile nodes are willing to forward packets for neighbours without any fixed infrastructure. Such networks have no fixed routers, since every node could be a router. All nodes are capable of moving and can be connected dynamically in an arbitrary manner. The responsibilities for organising and controlling the network are distributed among the nodes themselves.

Nodes form the ad hoc infrastructure necessary for cooperation, this ensures that multi-hop communication is achievable, allowing traffic from a node to reach its destination without requiring a significant amount of transmission energy, as in single hop communication, or simply to make transmission possible. However, for this to work means that nodes must be willing to forward traffic for other nodes, and in this way expend energy without receiving any direct gain from doing so. If a node considers its own short-term utility, then it may choose not to participate within the network.

A way to solve these problems is to introduce appropriate incentive mechanisms to encourage cooperative behaviour of selfish nodes.

The objective of this essay is to study the effect of mobility on the performance of ad hoc systems, where nodes have an incentive to collaborate. A mobility model should attempt to mimic the movements of real mobile nodes. Changes in speed and direction must occur, and they must do so in reasonable time slots.

This essay is organised as follows.

## Chapter 1

The concepts of mobile nodes and some mobility models used in performance evaluation of ad hoc network protocols are presented.

## Chapter 2

We propose a simple model of collective motion for an ad hoc network, using it to investigate the spatial dynamics of animal groups such as fish schools and bird flocks [7]. The mobility model assumes that the individuals move at constant speed, and that they adopt the average direction, subject to a random error, of the motion of the individuals in the local neighbourhood. This model is based on simple rules of avoidance, attraction and alignment.

## Chapter 3

A model for the operation of a mobile ad-hoc network where the nodes cooperate to form the necessary infrastructure that makes multi-hop communications possible is presented [13]. We simulate the model presented in section 4.3, where the movement of the nodes is determined by their own travel agendas. It is also influenced by their need to carry transit traffic in order to earn the credits necessary for them to transmit their own traffic. However, reception and transmission deplete the node's power, and the node may have to move to a location where it can recharge its battery.

## 2. Mobility Model for Ad Hoc Networks

### 2.1 Overview

A Mobile Ad Hoc network (MANET) is an autonomous system of mobile nodes connected by wireless links. In a MANET it is assumed that the nodes are free to move and are able to communicate with each other, often through multi-hop links, without the help of a fixed network infrastructure.

The network topology is dynamic. The movement of a node out of or into the communication range of other nodes changes not only its neighbour relationships with those other nodes, but also changes all routes based on those relationships.

Signalling overhead traffic for establishing and maintaining routes in a MANET is proportional to the rate of such link changes. Thus the performance of a MANET is closely related to the efficiency of the routing protocol in adapting to changes in the network topology and the link status [3],[21]

For the performance evaluation of a routing protocol for a MANET, it is imperative to use an appropriate mobility model to simulate the motion of the nodes in a network [14].

In this chapter we present some mobility models that have been proposed, or used in, the performance evaluation of Ad Hoc network protocols. The models presented are the random waypoint mobility model [3], the random Gauss-Markov model [24],[5], and the reference point group mobility model [9].

### 2.2 Random Waypoint Model

Johnson and Maltz describe the random waypoint (RWP) model in [12]. In this model, a node selects a random destination, uniformly distributed over a predefined region, and moves to that destination at a random speed, that is also uniformly distributed between a predefined minimum and maximum speed upon reaching the destination. After pausing for a certain period of time, the node selects a new random destination and speed.

A typical trajectory of a node moving in the random waypoint model is shown in figure 2.1

### 2.3 Random Gauss-Markov Model

The Random Gauss-Markov (RGM) Model was described by Sanchez [23] and was further developed by Liang and Haas [16]. In this model, each node is assigned a speed  $s$  and direction  $\theta$ , and these variables are updated at every time step  $\Delta t$  as follows,

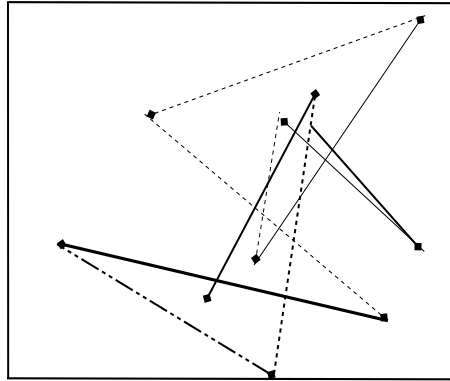


Figure 2.1: RWP model

$$s(t + \Delta t) = \min[\max(v(t) + \Delta v, V_{min}), V_{max}] \quad (2.1)$$

$$\theta(t + \Delta t) = \theta(t) + \Delta\theta \quad (2.2)$$

Here  $V_{min}$  and  $V_{max}$  are the minimum and maximum speeds of the node, and  $\Delta v$  and  $\Delta\theta$  are random variables uniformly distributed over the intervals  $[-\Delta v_{max}, \Delta v_{max}]$  and  $[-\Delta\theta_{max}, \Delta\theta_{max}]$ , respectively. When a node reaches a boundary, the node is reflected from that boundary by the selection of a new random direction. The update of  $s$  and  $\theta$  can be implemented in various ways. A typical trajectory of a node moving in a random Gauss-Markov Model is shown in figure 2.2.

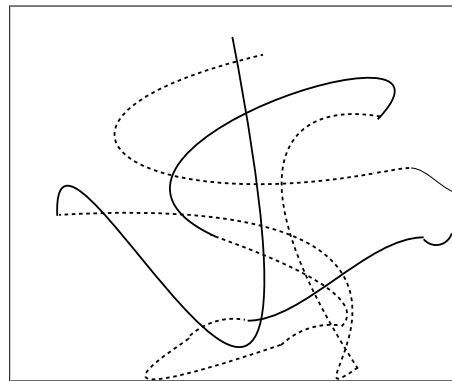


Figure 2.2: RGM model

## 2.4 Reference Point Group Mobility

The Reference Point Group Mobility (RPGM) model was described by Hong et al in [10]. In the RPGM model, each group of nodes has a logical centre, which defines characteristics of the group's motion such as location, speed and direction. Thus, the trajectory of a group is determined by the trajectory of its logical centre.

In addition to the logical centre, the RPGM model defines a reference point and a random motion vector for each node in the group. A reference point is a point about which a node moves at random with respect to the logical centre. The random motion vector represent the random deviation of a node from the reference point.

The random motion vector is updated periodically and its magnitude and direction are uniformly distributed over the intervals  $[0, RM_{max}]$  and  $[0, 2\pi]$  respectively. Let  $n(t_0)$  be the location vector of a node of the RPGM model at  $t = t_0$ , then

$$n(t_0) = c(t_0) + \overrightarrow{RP} + \overrightarrow{RM}(t_0), \quad (2.3)$$

Where  $c(t_0)$  denotes the location vector of the logical centre of the group at time  $t_0$ ,  $\overrightarrow{RP}$  is a vector from the logical centre to the reference point, and  $\overrightarrow{RM}(t_0)$  is the random motion vector. Then at  $t = t_0 + \tau$

$$n(t_0 + \tau) = c(t_0 + \tau) + \overrightarrow{RP} + \overrightarrow{RM}(t_0 + \tau), \quad (2.4)$$

For  $t_0 \leq t \leq t_0 + \tau$ ,  $n(t)$  is given by

$$n(t) = \frac{(t_0 + \tau - t)n(t_0) + (t - t_0)n(t_0 + \tau)}{\tau}, \quad (2.5)$$

A typical trajectory of a node moving in the RPGM model is shown in figure 2.3

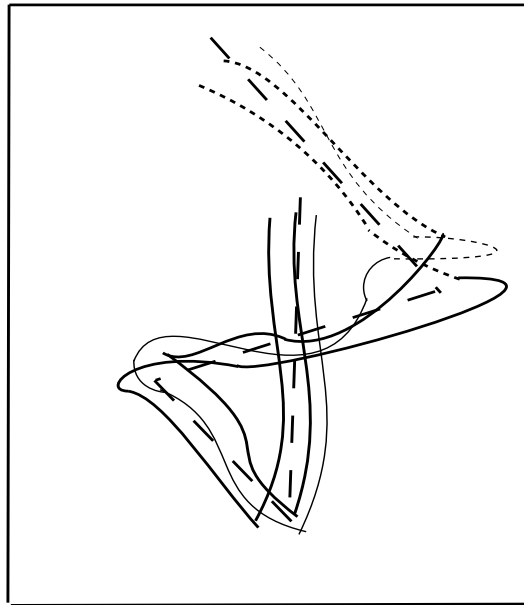


Figure 2.3: RPGM model (3 nodes)



Figure 2.4 depicts the movement of the RPGM model for a group with three nodes.

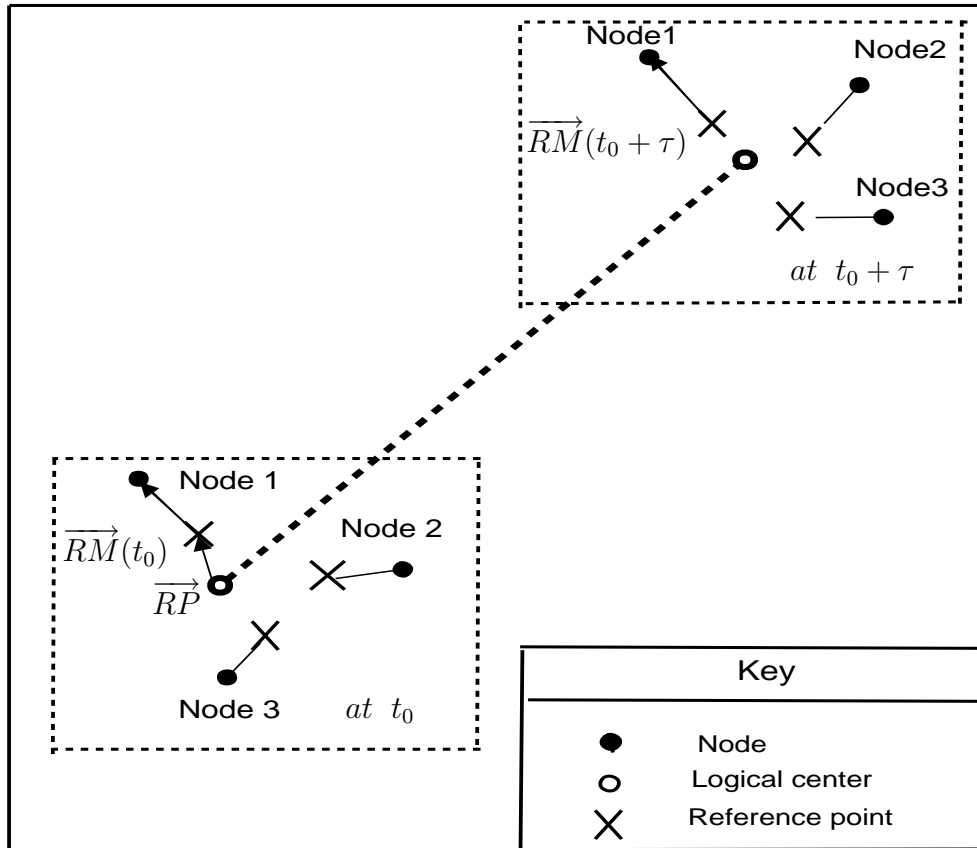


Figure 2.4: Description of RPGM model

At times  $t_0$  and  $t_0 + \tau$  the trajectory of the group is illustrated by superimposing the position of the nodes, their associated reference points and the group's logical centre, over time, on the same diagram.

For the purpose of clarity, only the vectors associated with node 1,  $\vec{RM}$  and  $\vec{RP}$ , have been labelled. It is useful at this point to recall that the  $\vec{RP}$  for a particular node remains constant throughout time.

## 2.5 Comments

Figures 2.1, 2.2 and 2.3 illustrate the typical travelling patterns of a mobile node(s) in the RWP, RGM, and RPGM models, respectively. Larger spacing between the dots indicates that higher speeds are involved.

---

The RWP model has a higher spatial node distribution at the centre of the network than near the boundaries [2], while the RGM model has a relatively uniform spatial node distribution over the entire network.

Moving at the same speed, an RWP node will travel farther than an RGM node over the same time interval, due to the travelling pattern.

Figure 2.3 illustrates a group of three nodes in the RPGM model with the logical centre moving according to the RWP model. Also shown is the trajectory of the logical centre of the group.

# 3. Biological Mobility Models

## 3.1 Overview

Our main objective in this chapter is to introduce and analyse a model of motion in an ad hoc network. The model must present a realistic account of the motion of the nodes. Some simple models already exist: the random waypoint model (RWP) and the random Gauss-Markov Model (RGM). These provide good descriptions of mobile nodes, but in reality, collision between nodes is impossible. In this chapter we introduce a new model, the Collective Motion Model, that forbids collisions between the nodes, yet maintains their grouping. As is common in the literature, we will use the term "individuals" to refer to mobile nodes.

## 3.2 The Model

In this model each individual attempts to maintain a minimum distance between itself and all the others at all times. The principal advantage of using this type of model is that collisions are avoided [7].

The model consists of  $N$  individuals ( $i = 1, \dots, N$ ), with vectors  $c_i$  representing each individual and unit direction vectors  $v_i$ .

The simulation is in three-dimensional space; time is discrete, with a time step,  $\tau$ , set to 0.1 seconds for example. For each time step, individuals evaluate the position or orientation or both, of the  $N$  neighbours with respect to the three behavioural zones described in figure 3.1. The actions that a particular individual takes will depend on the behavioural zone that it occupies.

The desired direction of motion for each individual  $d_i(t + \tau)$  is determined by the following rules.

Each individual attempts to maintain a minimum distance and avoid collisions with other members of the group within the zone of repulsion (ZOR), which is modelled as a spherical volume with radius  $r_r$ . If  $N_r$  neighbours are present in this zone (determined by the condition  $0 \leq |c_j(t) - c_i(t)| \leq r_r$  where  $c_j(t)$  is the position of the  $j$ -th neighbour individual,  $j = 1, \dots, N_r, j \neq i$ ) at time  $t$ , individual  $i$  responds by moving away from neighbours within this zone. We define

$$d_r(t + \tau) = - \sum_{j \neq i}^{N_r} \frac{r_{ij}(t)}{|r_{ij}(t)|} \quad (3.1)$$

$$r_{ij}(t) = \frac{c_j(t) - c_i(t)}{|c_j(t) - c_i(t)|}, \quad (3.2)$$

where  $r_{ij}(t)$  is the vector pointing from individual  $i$  in the direction of neighbour  $j$ . When  $N_r > 0$ , the preferred direction of the individual is

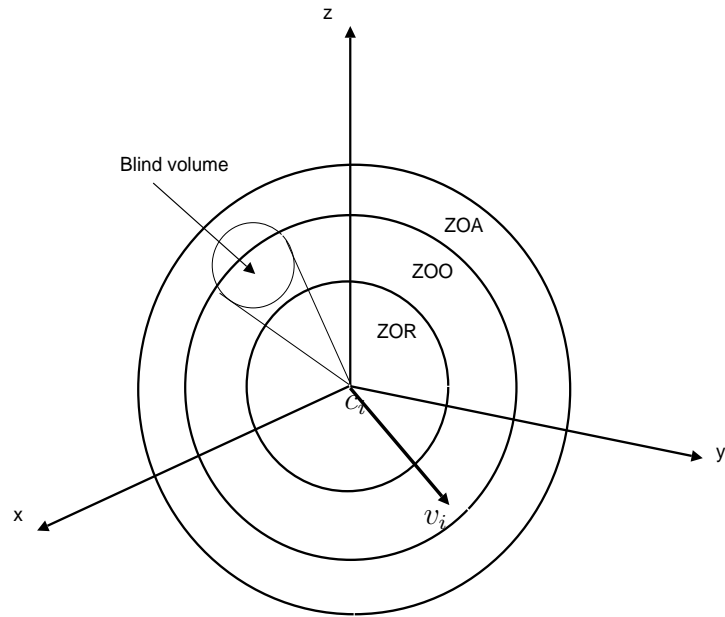


Figure 3.1: Representation of an individual in the model centred at the origin: ZOR=zone of repulsion, ZOO=zone of orientation, ZOA=zone of attraction. The possible "blind volume" behind an individual is also shown.

$$d_i(t + \tau) = d_r(t + \tau) \quad (3.3)$$

If there are no neighbours, present within the zone of repulsion (ZOR),  $N_r = 0$ , the individual  $i$  responds to neighbours within the zone of orientation and the zone of attraction, these zones are spherical (with radii  $r_o$  and  $r_a$ , respectively).

The zone of orientation (ZOO) contains  $N_o$  neighbours governed by the condition  $r_r \leq |c_j(t) - c_i(t)| \leq r_o$ . Likewise, there are  $N_a$  neighbours detectable in the zone of attraction (ZOA) such that  $r_o \leq |c_j(t) - c_i(t)| \leq r_a$  is satisfied.

We define  $\Delta r_o = r_o - r_r$  and  $\Delta r_a = r_a - r_o$  to be the widths of these zones.

The positions of the individuals within the zones of orientation and attraction are given respectively by :

$$d_o(t + \tau) = \sum_{j=1}^{N_o} \frac{v_j(t)}{|v_j(t)|} \quad (3.4)$$

$$d_a(t + \tau) = \sum_{j \neq i}^{N_a} \frac{r_{ij}(t)}{|r_{ij}(t)|} \quad (3.5)$$

If neighbours are only found in the zones of orientation (ZOO) ( $N = N_o$ ), then

$$d_i(t + \tau) = d_o(t + \tau). \quad (3.6)$$

Likewise, if all neighbours are found in the zone of attraction (ZOA),

$$d_i(t + \tau) = d_a(t + \tau). \quad (3.7)$$

If neighbours are found in both zones,

$$d_i(t + \tau) = \frac{1}{2} [ d_o(t + \tau) + d_a(t + \tau) ]. \quad (3.8)$$

In the rare case when the social forces cancel one another out and give a zero vector, or if no neighbours are detected, then

$$d_i(t + \tau) = v_i(t). \quad (3.9)$$

A blind volume is defined behind each individual such that in this area no neighbours can be detected. The blind volume is modelled as a cone with an interior angle  $(360 - \alpha)^\circ$ , where  $\alpha$  is defined as the field of perception.

Once the individuals have determined their desired directions of travel, they turn towards the direction vector  $d_i(t + \tau)$  by the turning rate  $\theta$ , provided the angle between the vector  $d_i(t + \tau)$  and  $v_i(t)$  is less than the maximum turning angle  $\theta_\tau$ . Then  $v_i(t + \tau)$  become  $d_i(t + \tau)$ . Otherwise, the individual rotates their current direction by  $\theta_\tau$  towards the desired travel direction.

To simplify the model we assume that each individual moves at a constant speed  $s$ , and at time  $t$  individual  $i$  at position  $c_i(t)$  travels with speed  $s$  in the direction  $v_i(t + \tau)$ . Between  $t$  and  $t + \tau$  the individual moves a distance  $\Delta = \tau s_i$ , updating the position at time  $t + \tau$ :

$$c_i(t + \tau) = c_i(t) + v_i(t + \tau)\Delta \quad (3.10)$$

A schematic diagram of the actions of individual  $i$  at each timestep in the model is shown in figure 3.2. [19]

### 3.3 Analysis of the Model

To analyse this model we need to define some descriptive statistics associated with direction. These statistics will be used to assess the global properties of a sample of directions

One fundamental statistic that we need to define is the centre of the group. The group centre is calculated as the mean of all the individual position vectors at time  $t$ :

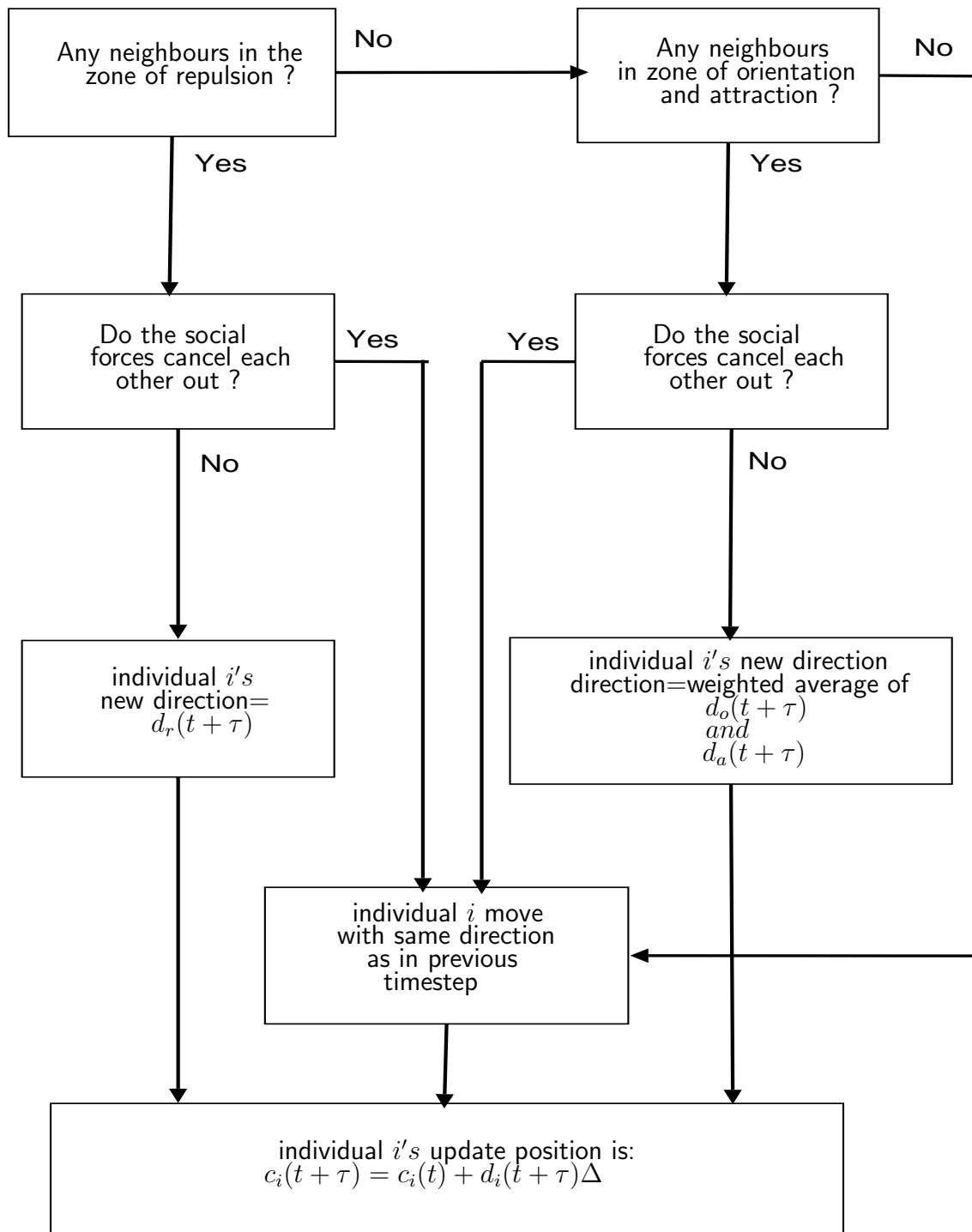


Figure 3.2: Schematic diagram of the algorithm used in the simulation of the deterministic collective motion model. The diagram is for individual  $i$  at position  $c_i(t)$  and moves in direction  $v_i(t)$  at time  $t$ . Each individual in the model performs these actions at every timestep.

$$c_{group} = \frac{1}{N} \sum_{i=1}^N c_i(t). \quad (3.11)$$

We introduce two global properties, calculated from the integrated trajectories of all the individuals.

The first property is called group polarisation  $p_{group}$  with  $0 \leq p_{group} \leq 1$ , and the second property is group angular momentum  $m_{group}$  where  $0 \leq m_{group} \leq 1$ .

The group polarisation increases as the degrees of alignment among individuals within the group increases.

The group angular momentum is the sum of the angular momenta of the individuals about the centre of the group,  $c_{group}$  (also known as the group centroid, 3.14)

Then

$$p_{group} = \frac{1}{N} \left| \sum_{i=1}^N v_i(t) \right| \quad (3.12)$$

$$m_{group} = \frac{1}{N} \left| \sum_{i=1}^N r_{ic}(t) \times v_i(t) \right| \quad (3.13)$$

where

$$r_{ic} = c_i - c_{group} \quad (3.14)$$

The group angular momentum measures the degree of the rotation of the group about its centre.

The individuals start with random orientation and at random positions; each individual can detect at least one other individual[22]. The collective behaviour of the model is measured after it reaches a dynamically stable state, where the values of the different systems measures have stabilised.

We introduce the direction vector  $d_{group}$  which extends from the group centre  $c_{group}$ ,

$$d_{group} = \frac{1}{N} \sum_{i=1}^N v_i(t). \quad (3.15)$$

This is used to define the plane perpendicular to  $d_{group}(t)$  that passes through  $c_{group}$ .

The individual at the front of the group is the one with the greatest minimum distance to the plane which  $d_{group}$  extends, whereas the individuals at the rear of the group have the greatest minimum distance from the plane. Other individuals are ranked accordingly (see figure 3.3).

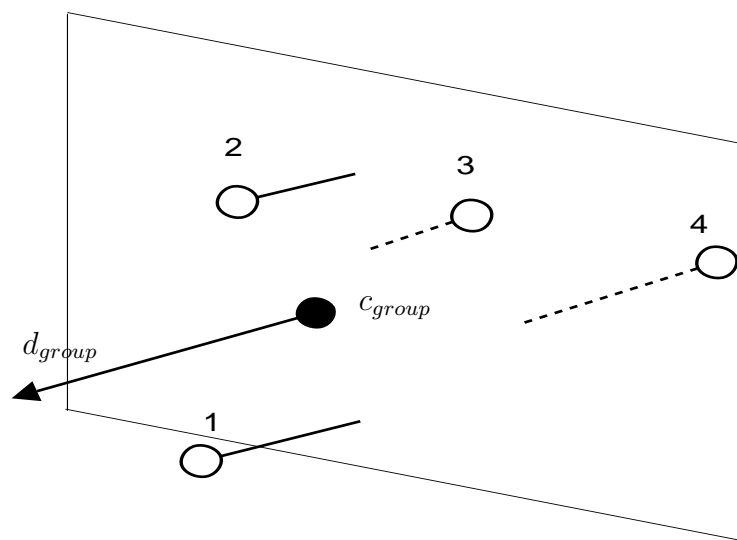


Figure 3.3: Measuring the order of four individuals within a group from the front. Individuals are represented as points relative to the group centre  $c_{group}$  with direction  $d_{group}$ . The plane is perpendicular to  $d_{group}$  and passes through the  $c_{group}$ . The shortest line segment between the plane and the individuals on the same side of the plane  $d_{group}$  (solid line). These individuals are in the front of the group. Those on the other side of the plane are shown as dotted lines, and are in the rear of the group. Note that all lines are parallel with  $d_{group}$ .



# 4. Incentives for Collaboration

## 4.1 Overview

In this chapter we introduce incentives for collaboration into the architecture of ad hoc networks, which will allow us to consider the dynamics of the cooperation and preference of nodes within a system.

This leads the use of pricing mechanisms, which have found application in rate control [8, 13, 17] and resource control [15, 18, 25] in wireless networks.

The difference in our case is that nodes recover the costs associated with energy losses and traffic loading at a particular node, through the credit arising from pricing mechanisms. This characteristic has been shown to stimulate cooperation within ad hoc networks [4].

Determining energy-efficient routes is also an important consideration in ad hoc networks [6, 26], and pricing mechanisms provide the means of guiding a system to its optimal operating point.

The dynamics of the system under consideration will be illustrated using a simulation model. In particular, we demonstrate the stability of price at nodes and their credit balances.

With regards to performance, we also investigate the throughput of the system. Certain dynamics of the system are also studied, including the arrival and departure of users from the system and how this effects the total credit. Finally, we consider how user mobility affects their individual throughput and also how it contributes to the overall system throughput.

In the final simulation, we look at the mobility, starting with a simple mobility model where only one node is in motion. After that we present another model where many nodes are in motion.

## 4.2 System Description

We model the network as a set  $N$  of mobile nodes that are equipped with directional antennas, with  $N = |N|$  being the number of nodes.

In this section we use term "node" to denote a topological entity which can be characterised in term of position, velocity, capacity constraint and routing, whereas the term "user" will refer to a person who desires to send traffic to the other users in the networks, in other words an active node.

### 4.2.1 Traffic Flow on Routes

Amongst the set of nodes  $N$ , we define a set  $S$  of sources and a set  $D$  of destinations to which traffic is sent. To do this, the set of routes between each source and destination pair has been

determined, where a route  $r \subset N$  is a subset of the nodes. These routes can be determined using routing protocols like AODV [20] or DSR [11].

Within the set  $R$  of routes within the networks, we can identify  $R^S(s)$  and  $R^D(d)$  as the subset of routes that originate at source  $s$  and the subset of routes that terminate at destination  $d$  respectively.

At a specific point of time, each source is transmitting a total amount of traffic  $x_s$ , which may be split among the routes  $r \in R^S(s)$ . Optimisation of the traffic flows, from a single source using multiple routes, has been considered previously [13, 26, 27].

The traffic flow along a particular route  $r$  is given by  $y_r$ , where  $y_r \geq 0$  and

$$x_s = \sum_{r \in R^S(s)} y_r. \quad (4.1)$$

## 4.2.2 Capacity Constraint

We consider nodes to be restricted to having one transceiver. We also observe that a node has limits on its capacity to transmit or receive traffic.

The total flow constraint can be modelled by calculating the total capacity usage, where traffic that is forwarded by a node should be both received and transmitted.

$$c_j = \sum_{r \in R^S(j) \cup R^D(j)} y_r + \sum_{\substack{r: j \in r \\ r \notin R^S(j) \cup R^D(j)}} 2y_r, \quad (4.2)$$

and capacity usage is constrained as follows

$$c_j \leq C_j, \quad \forall j \in N, \quad (4.3)$$

where  $C_j$  is the total capacity of node  $j$ . Notice that this constraint is a simplification that ensures that a node cannot receive traffic from, or transmit traffic to, two of its neighbours simultaneously.

## 4.2.3 Energy Management

A key issue within mobile ad hoc networking is energy efficiency, and this can be achieved through traffic management and optimal routing of traffic flows.

The energy consumed per unit flow when transmitting traffic from node  $i$  to node  $j$  is represented by the variable  $e_{ij}^{(tx)}$ .

Receiving data also consumes energy, so we present this energy consumption by the constant  $e^{(rx)}$ .

Note that if the node  $j$  cannot be reached from node  $i$ , then  $e_{ij}^{(tx)} = \infty$ . We use the notation  $f_{ri}$  for the node that  $i$  will forward traffic to, when using route  $r$ .

The power consumed by node  $j$  is :

$$\gamma_j = \sum_{r \in R^S(j)} y_r e_{j f_{rj}}^{(tx)} + \sum_{r \in R^D(j)} y_r e^{(rx)} + \sum_{\substack{r: j \in r, \text{ and} \\ r \notin R^S(j) \cup R^D(j)}} y_r (e^{rx} + e_{j f_{rj}}^{(tx)}). \quad (4.4)$$

Power consumption is constrained at a node, due to the rate of discharge of the node's battery. This leads us to the following power constraint at each individual node:

$$\gamma_j \leq \Gamma_j, \quad \forall j \in N, \quad (4.5)$$

where  $\gamma_j$  depends on the specification of the node's power supply.

## 4.3 Model

### 4.3.1 Dual Algorithm for Flow Allocation

We define the model by assuming that each user  $s$  has a willingness-to-pay parameter  $w_s(t)$ , and the user adjusts its flow rate on each route  $r$  (where  $r \in R^S(s)$ ) as a function of time, so that the total flow rate generated by user  $s$  is given according to the expression

$$x_s(t) = \sum_{r \in R^S(s)} y_r(t) = \frac{w_s(t)}{\min_{r \in R^S(s)} \sum_{j \in r} \mu_{jr}(t)}, \quad (4.6)$$

with  $y_r$  only being positive on routes  $r$  that attain the minimum in the denominator.

The variable  $\mu_{jr}(t)$  is the price that node  $j$  charges for forwarding a unit flow along route  $r$ .

This model closely reflects what occurs in a mobile ad hoc network, as the lowest cost paths will be selected in practice.

Prices along the routes are defined according to the following equation:

$$\mu_{jr}(t) = \begin{cases} e_{jfrj}^{(tx)} \mu_j^P(t) + \mu_j^B(t), & j \text{ is the source node on route } r, \\ (e_{jfrj}^{(tx)} + e^{(rx)}) \mu_j^P(t) + 2\mu_j^B(t), & j \text{ is a transit node for route } r, \\ e^{(rx)} \mu_j^P(t) + \mu_j^B(t), & j \text{ is the destination node on route } r. \end{cases} \quad (4.7)$$

where the congestion prices  $\mu_j^P(t)$  and  $\mu_j^B(t)$ , for power and bandwidth, respectively, are dynamically adapted according to the equations

$$\frac{d}{dt} \mu_j^B(t) = \frac{\kappa \mu_j^B(t)}{C_j} (c_j(t) - C_j) \quad (4.8)$$

and

$$\frac{d}{dt} \mu_j^P(t) = \frac{\kappa \mu_j^P(t)}{\Gamma_j} (\gamma_j(t) - \Gamma_j). \quad (4.9)$$

The dependence of the right-hand sides of 4.8 and 4.9 on both the current price and the respective capacities is an attempt to scale the dynamics of the price in a network with widely differing prices and capacities. The overall effect of this dual algorithm is, under stable operation, to allocate flows to routes for each user in such a way that the traffic for a given user  $s$ , say, faces congestion cost at the rate of  $w_s(t)$  per unit time.

The global stability of the system (4.6-4.9) can be established by the construction of an appropriate Lyapunov function [13], in the case where the network structure is static. We investigate here a model where both the network structure and the set of sources is varying over time.

### 4.3.2 Balancing the Congestion Costs

We suppose that each user maintains a credit balance,  $b_s(t)$ , which receives an initial endowment of 1 when the user arrives into the system, where we here identify a node with the user,  $s$ , say, whose routes originate at that node.

The user's credit balance is then adjusted by transferring credit equal to the congestion costs to each of the downstream resources.

Each user will seek to control its credit balance  $b_s(t)$  and we envisage them doing so by dynamically adjusting their willingness-to-pay parameters  $w_s(t)$  according to the level of their credit balance, for some parameter  $\alpha_s > 0$ , by following a rule of the form:

$$w_s(t) = \alpha_s b_s(t) \quad (4.10)$$

In this way, the user's sending rates become coupled with their credit balance, and they would thereby naturally reduce their sending rate whenever their credit was low.

The credit balance itself is discounted over time

$$\frac{db_s}{dt} = -\beta(b_s(t) - 1) - w_s(t) + \sum_{r:s \in r} y_r \mu_{sr}(t) \quad (4.11)$$

where  $\beta$  is a small position constant.

This will tend to keep the sum of the credit balances  $b_s(t)$  over all sources  $s \in N$  (the total credit in the system) near the population size  $N$ : when a user leaves the system, the total credit in the system will adjust towards the size of the remaining population.

## 4.4 Simulations

We define our network to consist of ten users located randomly, and according to a uniform distribution, within a geographical area of  $100m$  by  $100m$ , as shown in figure 4.1. This allows us to study a set of nodes with diverse geographical locations and topological relationships.

Each node is equipped with a single transceiver with a range of 56 meters, which defines its set of neighbours. Note that nodes in the centre of the network, such as  $N_8$ , have a large set of neighbours, hence a higher number of routes which they can use to send traffic to a particular destination.

Nodes such as  $N_1$  and  $N_2$  have only a few neighbours; they can only select a restricted number of routes to send traffic to a particular destination.

In this simulation we assume that each user establishes a connection with a randomly selected recipient, and the duration of this connection is exponentially distributed. Also, once the connection with a particular destination node terminates, the user stays idle, for an exponentially distributed period, before randomly selecting another node with which to initiate a connection.

When a user initiates a connection with another user, it determines the lowest cost route and then uses that route for the duration of the connection. Notice that this is a departure from the model described in section 4.3, where users continually monitor all available routes to the recipient user and always send traffic through the route with minimum cost.

However, this departure from the model is a realistic one, because we want to minimise the amount of routing information that has to be distributed within the network. When using one of the ad hoc routing protocols, such as AODV [20] or DSR [11], it is reasonable to assume that the integrity of routes will need to be checked before routing a stream of packets along a particular path. However, it is unlikely that nodes will continuously monitor all paths at the granularity level of transmitting each packet.

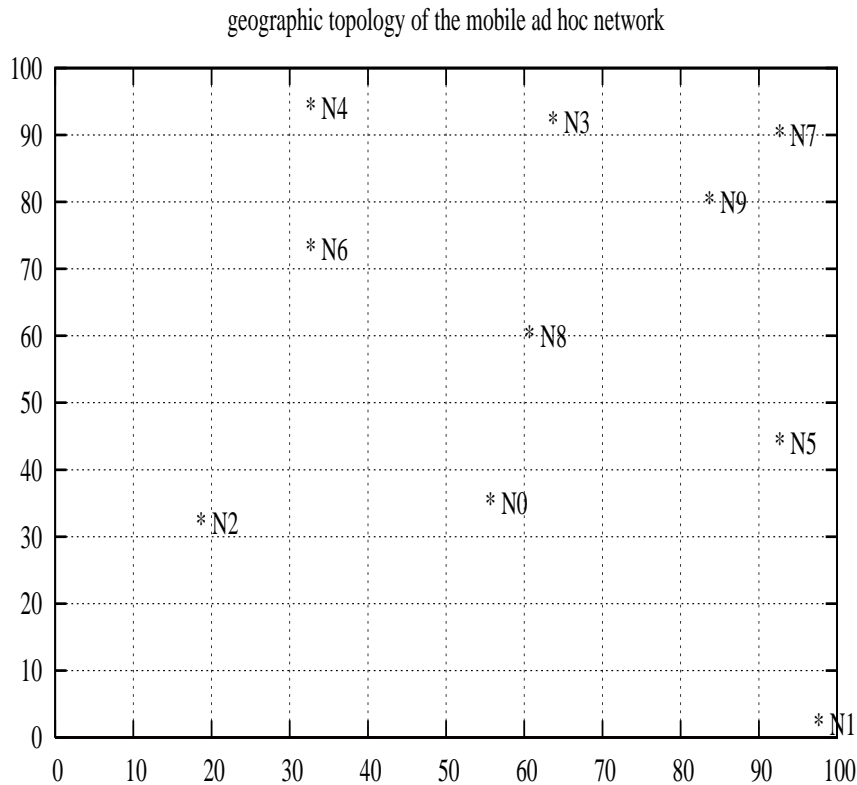


Figure 4.1: Topology of the mobile ad hoc network.

A consequence of this deviation from the original model is that the system will not achieve optimal performance. The motivation for applying such a change is that there is a trade-off between optimality and the overhead involved in continuously monitoring the prices of other routes to the destination.

Another advantage of this approach is that route-flap, which may occur if the price of another route drops below that currently being used, resulting in users frequently swapping traffic between these two routes.

#### 4.4.1 Static Networks

In this section we begin by demonstrating the stability of the system. We simulate a static network topology over  $10,000s$ , with a mean of  $0.5s$  for the connection time, and the user is idle for the same duration after completing the connection. Users update their prices every  $0.01s$ . The system parameters are given by  $\alpha_s = 0.3$ ,  $\beta = 0.01$  and  $\kappa = 0.05$ . The value of the bandwidth capacity  $C$  is 7.5 for all nodes in the network, and the maximum power  $\Gamma$  is equal to 0.5. The energy parameters associated with transmitting and receiving traffic are given by  $e_{ij}^{(tx)} = 10^{-4} \|z_i - z_j\|_2^2$  and  $e^{(rx)} = 10^{-3}$ , where  $z_i$  and  $z_j$  are the geographical position of nodes  $i$  and  $j$ , respectively.

The bandwidth and power price of four nodes in the network are shown in figures 4.2 and 4.3, respectively. Figure 4.1 indicates the positions of the nodes in the network. Node  $N_1$  is the most extreme node in the network, node  $N_7$  is also an extreme node though nodes  $N_3$  and  $N_9$  are very close to it.

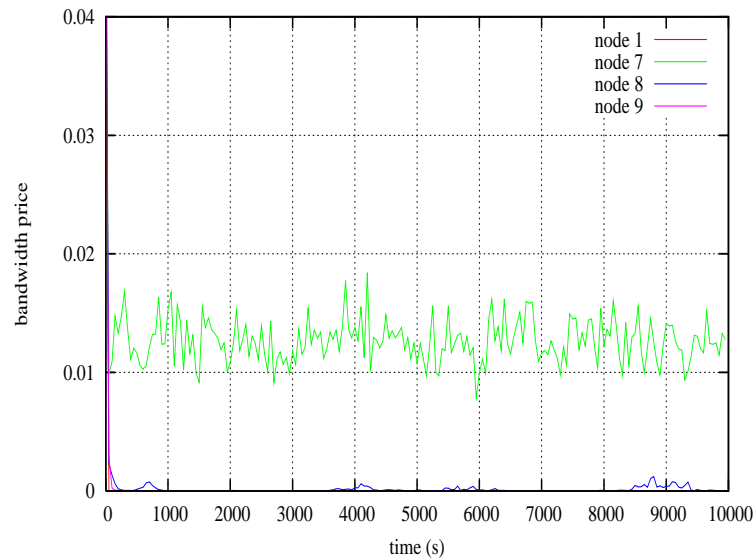


Figure 4.2: Bandwidth prices of four nodes  $N_1$ ,  $N_7$ ,  $N_8$  and  $N_9$ .

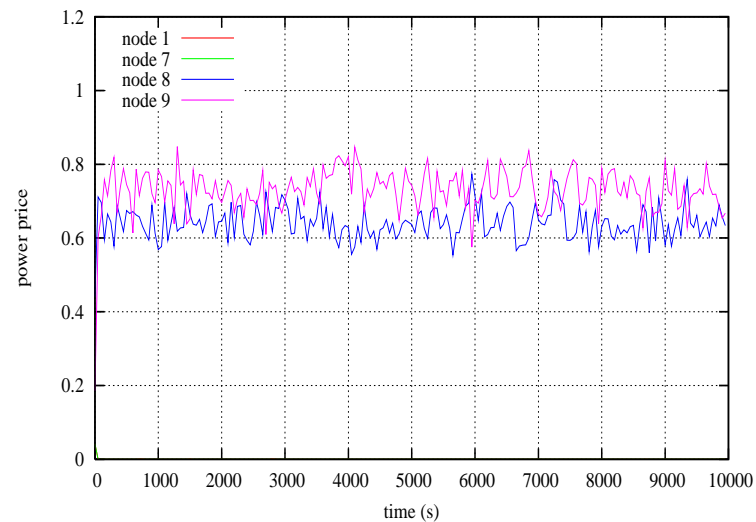


Figure 4.3: Power prices of four nodes  $N_1$ ,  $N_7$ ,  $N_8$  and  $N_9$ .

From these plots, we can observe that each price (bandwidth, power) stabilises about its mean value, hence proving that the overall system is stable. It should be noted that this occurs for the sub-optimal routing policy where minimum cost routes are only selected when connections are established.

A second observation is that all the prices for node  $N_1$ , which is on the edge of the network, decay

rapidly to zero. This is because no routes use  $N_1$  as a transit node, and flows which consume bandwidth or power resources at this node are those originating or terminating at  $N_1$ .

It is also interesting to observe the price of nodes  $N_8$  and  $N_9$ . The power price is high for both  $N_8$  and  $N_9$ . The reason for this is that node  $N_8$  is close to the centre of the network, where distances to its neighbour nodes are relatively high, so more power is consumed by  $N_8$  in transmitting to other nodes. However, node  $N_9$  is not centrally located on the network, but is close to nodes  $N_3$  and  $N_7$ , so node  $N_9$  will be carrying larger amounts of traffic for these nodes and others, resulting in its high power consumption.

The credit balances and throughput, for the same nodes, are also plotted in figures 4.4 and 4.5, respectively.

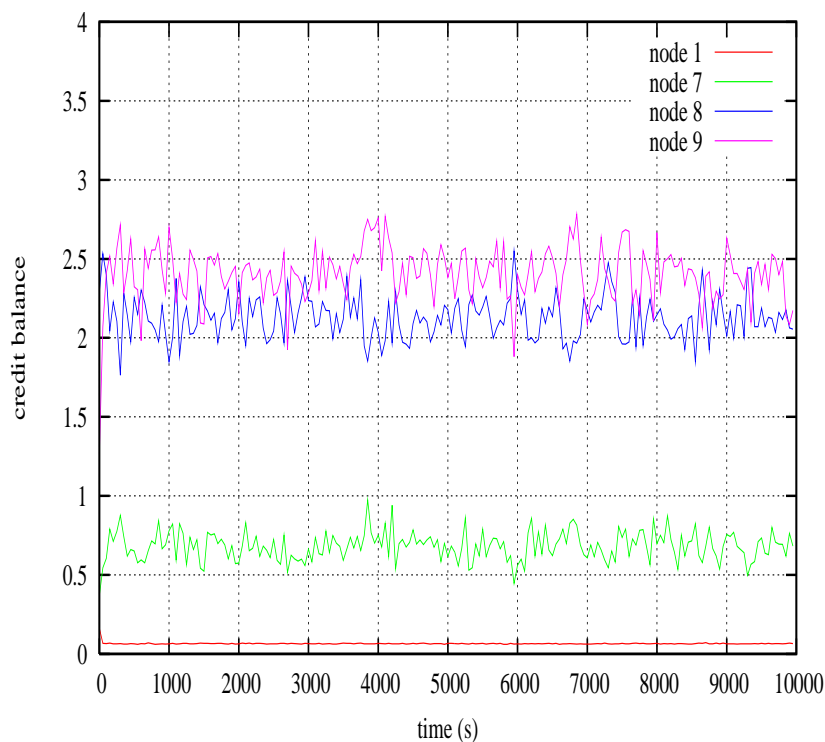


Figure 4.4: Credit balance of four nodes ( $N_1$ ,  $N_7$ ,  $N_8$ , and  $N_9$ ).

The throughput is determined by logging the accumulated traffic originating from the nodes. We again note that these quantities stabilise around their associated means. The mean value for each node's credit balance is largely dependent on its geographical location within the network. We expect that nodes  $N_8$  and  $N_9$  will maintain the highest credit balance, as they will be carrying a large amount of transit traffic.



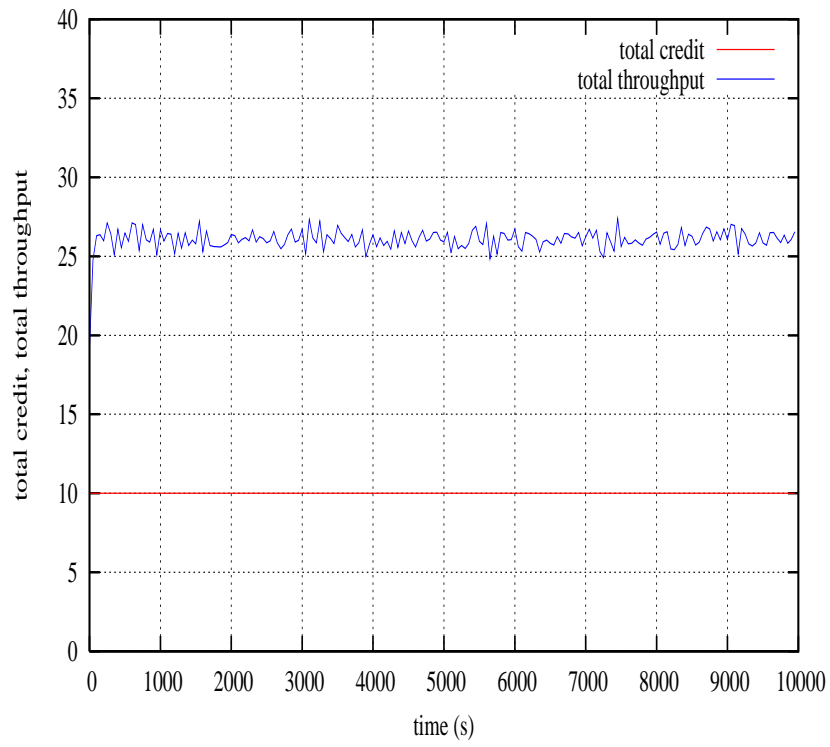


Figure 4.5: Total throughput and total credit.

### 4.4.2 Mobile Networks

The objective of this essay is to study the effect of mobility on the performance of an ad hoc network, where nodes have a built-in incentive to collaborate. In this section we return to the original topology considered in figure 4.1, where the node  $N_1$  is mobile and follows the path shown in figure 4.6, through the geographical centroid of the static network.

Node  $N_1$  moves across the network and reaches the other edge of the network by the end of the simulation after  $10^5$  seconds of simulated time. To reach this final location node  $N_1$  moves with a velocity of  $(-57 \times 10^{-5}, 98 \times 10^{-5})m/s$ .

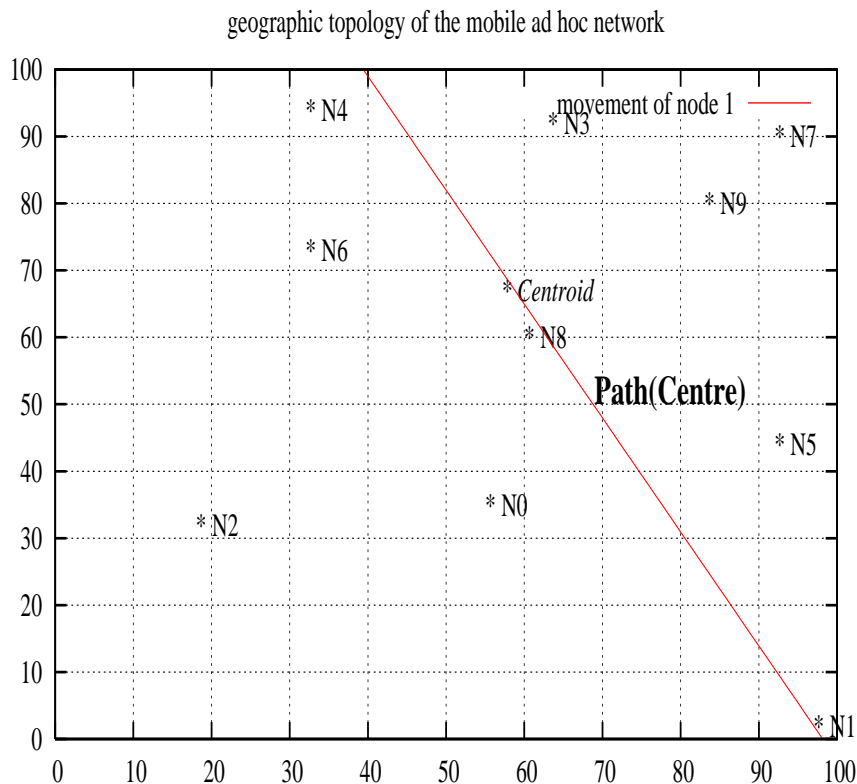


Figure 4.6: Path of node  $N_1$  through the network.

When node  $N_1$  approaches the network centre, it will be used more frequently as a transit node to carry traffic between other nodes. This can be observed from figures 4.7 and 4.8, which show that the bandwidth and the power price of node  $N_1$  increase when it is near the centre. At the same time, other nodes have a choice to send traffic through either  $N_1$  or  $N_8$ .

Node  $N_1$  affects the power price of node  $N_8$ ; it helps to reduce it. As node  $N_1$  moves away from the centre of the network, these effects on the node power and bandwidth price subside.

The increase in the prices associated with node  $N_1$ , when it is near the centre of the network, and its increased traffic load which is forwarded to other nodes, means that its credit balance also grows, as shown in figure 4.9. This increases the ability of node  $N_1$  to generate traffic, as its

willingness-to-pay is related to its credit balance. Consequently, its total throughput increases, and we can observe this in figure 4.10.

The increase in throughput and bandwidth price, when the node moves closer to another node, is also observed when  $N_1$  moves away from the centre of the network and close to node  $N_4$ . A comparison of figures 4.5 and 4.10 indicates that the overall total throughput within the network increases when node  $N_1$  moves to the centre of this network. In comparison, when  $N_1$  moves away from the centre to the edge, the overall total throughput decreases.

Thus our results indicate ways in which the overall performance varies with the current geographical distribution of the users. Moreover, mobile users can influence not just their own performance, but also the overall performance of the network.

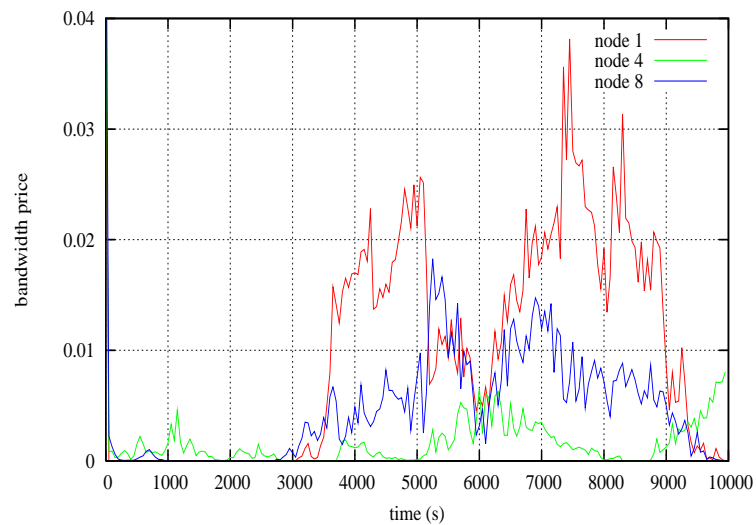


Figure 4.7: Bandwidth price of the mobile node  $N_1$ , and two stationary nodes  $N_4$  and  $N_8$

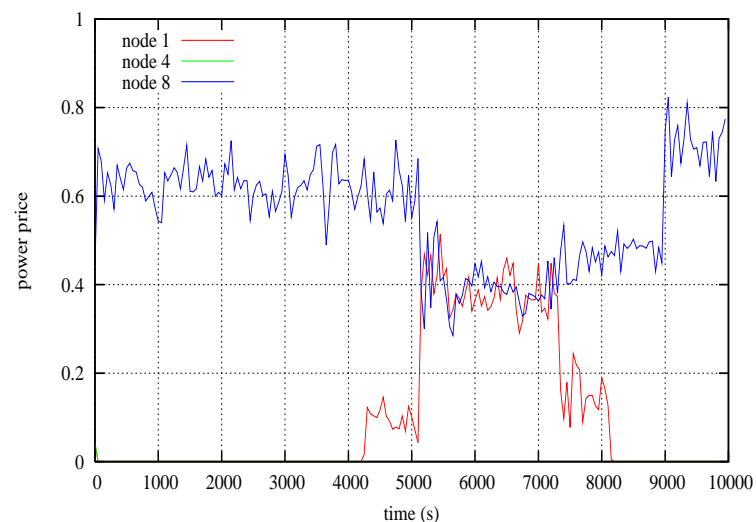


Figure 4.8: Power price of the mobile node  $N_1$ , and two stationary nodes  $N_4$  and  $N_8$

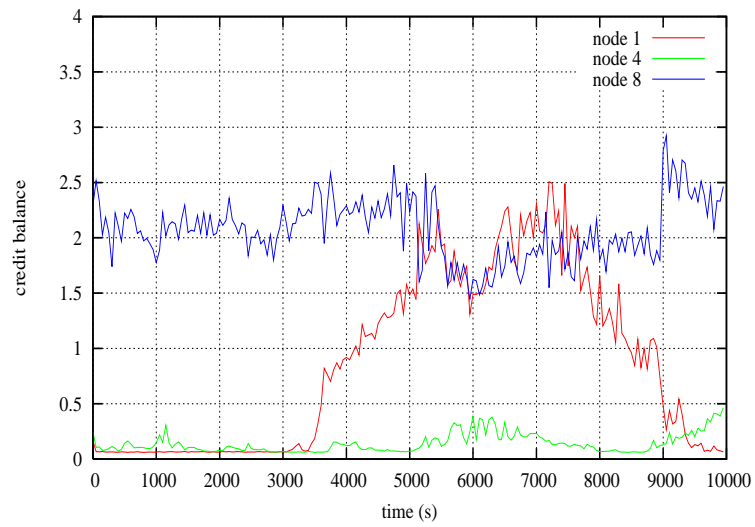


Figure 4.9: Credit balance of the mobile node  $N_1$ , and two stationary nodes  $N_4$  and  $N_8$

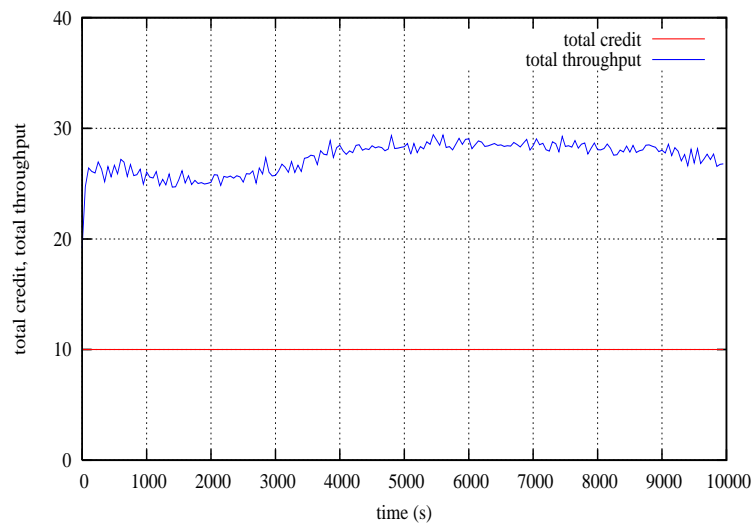


Figure 4.10: Total throughput and total credit

### 4.4.3 Autonomous Network

The final objective of this essay is to define another type of mobility model, that of autonomous motion, to simulate the case where each node moves in order to maximise its credit balance.

We return to the original topology considered in figure 4.1, where every node moves with a velocity of  $200 \times 10^{-5}, 200 \times 10^{-5})m/s$ ,

When the nodes start moving to the centre of the network, each node maintains a minimum distance between itself and other nodes.

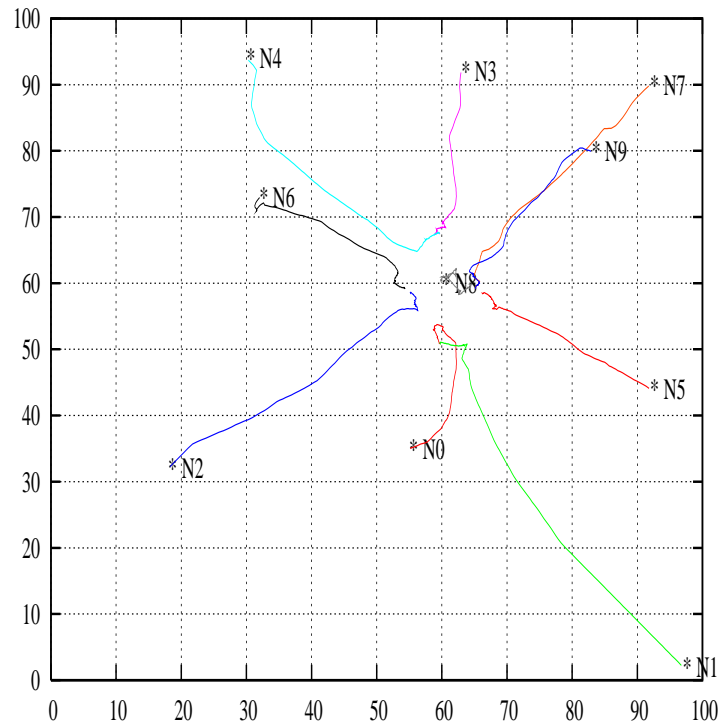
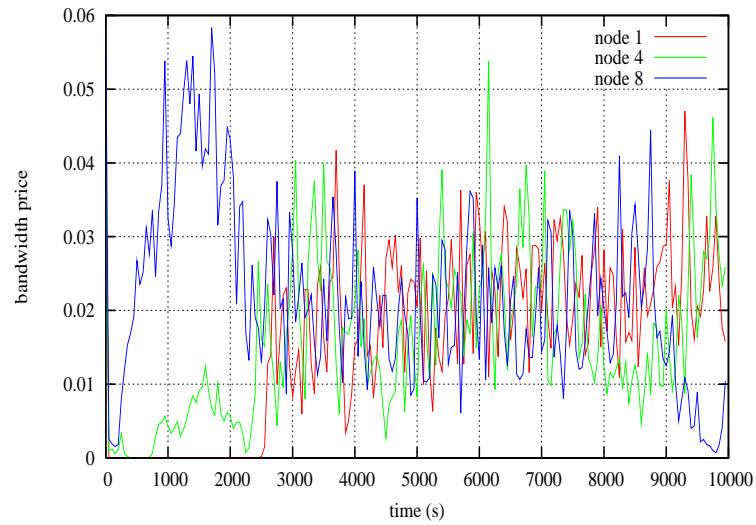
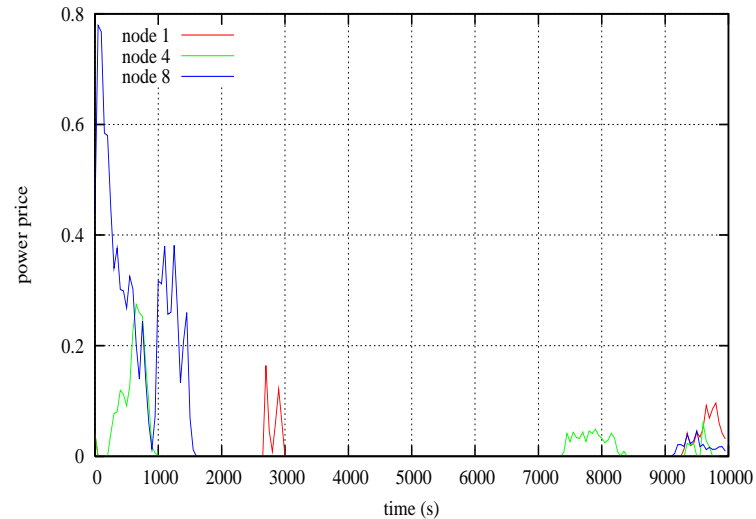


Figure 4.11: Path of nodes through the network.

As they approach the centre of the network, the bandwidth price of nodes  $N_1$  and  $N_4$  start to increase, and correspondingly decrease for node  $N_8$ . This occurs because  $N_1$  and  $N_4$  move to the centre, and the distance between all the nodes decreases. When they reach the neighbourhood of the centre, each node maintains a distance between itself and all other nodes of less than  $56cm$ . The bandwidth price for each node stabilises about the same mean value, and this can be observed from figure 4.12.

Around the centre of the network, each node can send traffic to the destination without any help from transit nodes. The power price then decays to zero for all nodes; Figure 4.13 indicates this.

Figure 4.12: Bandwidth price of the mobile nodes  $N_1$ ,  $N_4$  and  $N_8$ Figure 4.13: Power price of the mobile nodes  $N_1$ ,  $N_4$  and  $N_8$ 

The credit balance and total throughput, for the same nodes, are presented in figures 4.14 and 4.15, respectively. During the first run of the simulation, node  $N_8$  has the highest credit balance, as it will be carrying a large amount of transit traffic; the opposite is true for node  $N_1$ . When all nodes move to the centre of the network, the credit balance increases for all of them. This helps to decrease the credit balance for  $N_8$ .

Around the centre, every node stabilises around the same mean value credit balance. Figure 4.15 indicates that total throughput has stabilised around its mean value.

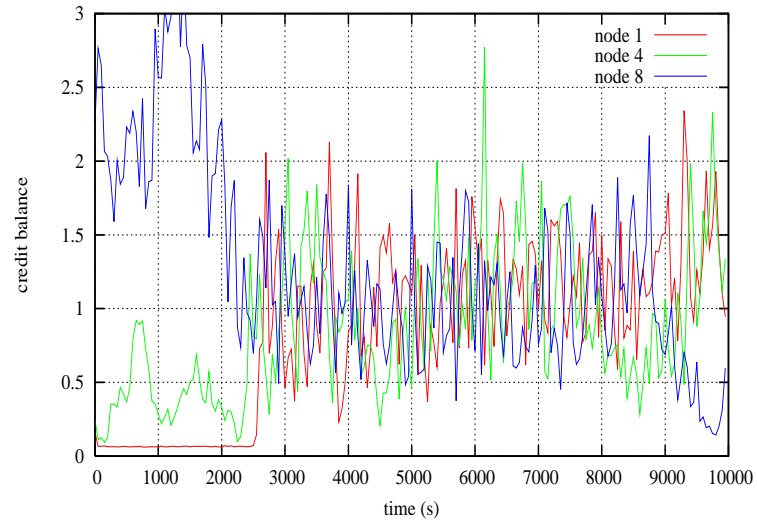


Figure 4.14: Credit balance of the mobile nodes  $N_1$ ,  $N_4$  and  $N_8$

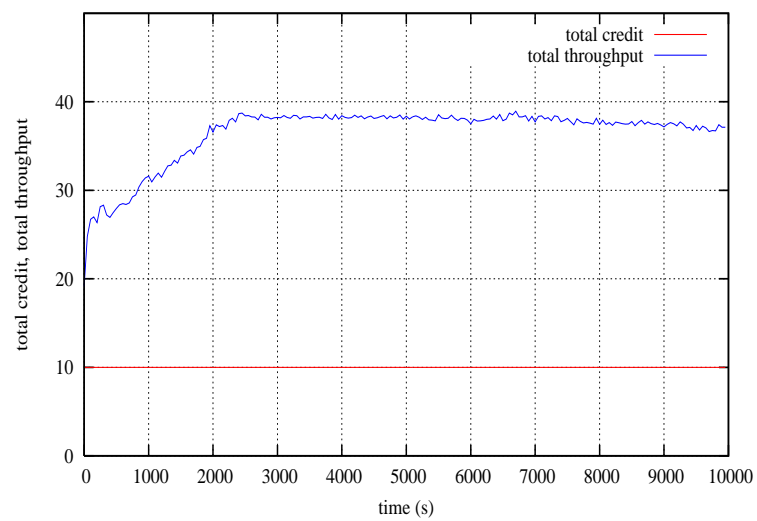


Figure 4.15: Total throughput of the mobile nodes

## 5. Conclusion

We have presented how to integrate incentives for collaboration into the operations of a mobile ad hoc network, so that the cost of resources consumed at transit nodes, when the nodes forward the traffic along multi-hop routes, can be recovered using pricing mechanisms.

These prices are determined in an algorithmic fashion, where the base of the algorithms used by individual users to update their prices, is their bandwidth and power usage. Routes for connections from a user to a particular destination are chosen such that the route price is minimal. This leads to the dual algorithm for traffic management within the network.

The mobility of a node is first investigated by allowing a single node to move through the centre of the network. We generalise this motion to other motion models, specifically, an autonomous motion model where all nodes can move.

In this essay, we have studied the system shown in section 4.3, through simulation. These simulations demonstrate that the user's bandwidth price, power price and credit balance all stabilise for a static ad hoc network, and we also presented the advantages of being near the centre of the network, as this allows the nodes to act as transit nodes for a larger number of routes.

The final part of the simulation allows all the nodes to move autonomously, and demonstrates that the power price decays to zero and increases the total throughput of the system when all nodes are near the network centre.

Our simulations show that the model we presented in section 4.3 captures many of the fundamental trade-offs within the collaborative setting of a mobile ad hoc network.



# Acknowledgements

I would like to express my profound gratitude to my supervisor prof. AE Krzesinski for his support, guidance and encouragement. Acknowledgement is also made to Prof. K Belarbi.

I wish also to make a special mention of Anahita and Christian my tutors who really helped me greatly. I would like to acknowledge all AIMS lecturers, tutors and staff especially, Prof Fritz Hahne, Prof Neil Turok and Igsaan Kamalie for giving me the opportunity to learn from them.

I acknowledge the AIMS 2006 students for the special time we have spent together and more especially the wonderful experiences that I have had from them because they have really affected my life.

To every one of you, I say

شكراً

# Bibliography

- [1] Alan F. Beardon. From problem solving to research, 2006. Unpublished manuscript.
- [2] C. Bettstetter and C. Wagner. The spatial node distribution of the random waypoint mobility model. *Proc. 1st German Workshop on Mobile Ad-Hoc Network (WMAN'02)*, pages pp.41–58, Ulm, Germany, March 2002.
- [3] J. Broch, D.A. Maltz, D.B. Johanson, Y. c. Hu, and J. Jetcheva. A performance comparison of multi-hop wireless ad hoc network routing protocols. *IEEE/ACM, Mobicom'98*:pp.16–28, 1998.
- [4] L. Buttyan and J. P. Hubaux. Stimulating cooperation in self-organizing mobile ad hoc networks. *ACM/Kluwer Mobile Networks and Application*, 8(5), October 2003.
- [5] T. Camp, J. Boleng, and V. Davies. A survey of mobility for ad hoc network research. *Wireless Communication and Mobile Computing (WCMC): Special issue on Mobile Ad Hoc Networking: Research, Trends and Applications*, pages pp.483–502, 2002.
- [6] J. H. Chang and L. Tassiulas. Energy conserving routing in wireless ad-hoc networks. *Proceeding of INFOCOM'00*,, March 2000.
- [7] Iain D. Couzin, Jens Krause, Richard James, Graeme D. Ruxton, and Nigel R. Franks. Collective memory and spatial sorting in animal groups. *Elsevier Science*, 2002.
- [8] R. J. Gibbens and F. P. Kelly. Resource pricing and the evolution of congestion control. *Automatica*, 35:1969–1985, 1999.
- [9] X. Hong, M. Gerla, G. Pei, and C.-C. Chiang. A group mobility model for an ad hoc wireless network. *Proc.ACM/IEEE, MSWiM'99*:pp.53–60, 1999.
- [10] Xiaoyan Hong, Mario Gerla, Guangyu Pei, and Ching-Chuan Chiang. A group mobility model for ad hoc wireless networks, August 1999. in *Proceedings of the ACM International Workshop on Modeling and Simulation of Wireless and Mobile Systems (MSWiM)*.
- [11] D. Johnson and D. Tse. The dynamic source routing protocol for mobile ad hoc networks (**DSR**), February 2002. IETF internet Draft draft-ietf-manet-dsr-07.txt.
- [12] David B. Johnson and Daviv A. Maltez. Dynamic source routing in ad hoc wireless networks. *in Mobile Computing. Kluwer Academic Publishers*, pp:153–181, 1996.
- [13] F. P. Kelly, A. K. Maulloo, and D. K. H. Tan. Rate control for communication networks: Shadow prices, proportional fairness and stability. *Journal of the Operational Research Society*, 49(3):237–252, March 1998.
- [14] Byung Jae Kwak, Nah-Oak Song, and Leonard E. Miller. A standard measure of mobility for evaluating mobile ad hoc network performance. *IECE TRANS. COMMUN*, E86-B, 2003.

- 
- [15] R. Liao, R. Wouhaybi, and A. Campbell. Incentive engineering in wireless **LAN** based access networks. *Proceedings of ICNP 2002*, November 2002.
- [16] B Ling and Z. Haas. Personal communication. February 4 2000.
- [17] S. Low and D. Lapsley. Optimisation flow control **I**: algorithm and convergence. *IEEE/ACM Transactions on Networking*, 7(6):861–874,, December 1999.
- [18] P. Marbach and R. Berry. Downlink resource allocation and pricing for wireless networks. *Proceedings of INFOCOM'02*, June 2002.
- [19] Merrifield and James, editors. *An Investigation Of Mathematical Models For Animal Group Movement, Using Classical And Statistical Approaches*. Number 133. University of Sydney. School of Mathematics and Statistics.
- [20] C. Perkins, E. Belding-Royer, and S. Das. Ad hoc on-distance vector (**AODV**) routing, November 2002. IETF internet Draft draft-ietf-manet-aodv-12.txt.
- [21] C.E. Perkins, E.M. Royer, S.R. Das, and M.K. Marina. Performance comparison of two on-demand routing protocols for ad hoc networks. *IEEE Pers. Commun.*, vol.8, no.1, pp16-28, 2001.
- [22] W. H Press, Teukolsky, W. A. Vetterling, W. T., Flannery, and B. P. Numerical recipes in **C**. *the Art of Scientific Computing*, 2nd Edn, 1992.
- [23] Miguel Sanchez. Node movement models in ad hoc networks, July 15, 1999. IETE MANET Mailing List.
- [24] D. Shukla. *Mobility models in ad hoc networks*. Master's thesis, KReSIT-ITT Bombay, Nov. 2001.
- [25] Vasilios Siris. Resource control for elastic traffic in **CDMA** networks. *Proceeding of MOBICOM'02*,, September 2002.
- [26] V. Srinivasan, C. Chiasserini, P. Nuggehalli, and R. Rao. Optimal rate allocation and traffic splits for energy efficient routing in ad hoc networks. *Proceedings of INFOCOM'02*,, June 2002.
- [27] W. H. Wang, M. Palaniswami, and S. Low. Optimal flow control and routing in multi-path networks, October 2002. Preprint submitted to Performance Evaluation.